EXPERIMENTAL VALIDATION OF AN ANALYTICAL MODEL FOR O-RING FRICTION AND LEAKAGE AT HIGH PRESSURE

Andres Campos
Department of Mechanical Engineering,
University of Minnesota
111 Church Street SE, Minneapolis, MN, 55455
Email: campo074@umn.edu

William K. Durfee
Department of Mechanical Engineering,
University of Minnesota
111 Church Street SE, Minneapolis, MN, 55455
Email: wkdurfee@umn.edu

ABSTRACT

The objective of this study was to validate existing analytical models of the friction force and leakage for O-ring seals at high pressure, where high pressure is defined as 2000 psi. A set of three pistons with 9, 6, and 4 mm bore were used in this experiment. Each piston had a single O-ring seal located in the cap end. To validate the friction force model, the force efficiency was measured by exerting a load on a piston and collecting pressure, load, and displacement measurements during constant piston descent. To validate the leakage model, a static leakage test was performed by measuring the displacement of the piston after being exposed to a constant load for an extended amount of time. Results indicated that the friction force efficiency model was valid for a range of pressures between 500 and 2000 psi, which indicates that the model for O-ring friction holds at high pressure. Results from the leakage test showed that the piston moved close to 600 microns during the first 12 hours of testing and did not move for the remaining 36 hours. This indicates that O-ring seals are leak-free, so the volumetric efficiency can be approximated to be 100%. Simple O-ring seal models can be used to compute the overall efficiency of small-scale hydraulic systems at high pressure.

INTRODUCTION

Hydraulic actuation is widely used for high force, speed, and power applications such as in construction machinery [1], and recent efforts have focused in using this technology for small-scale applications. While the efficiency of large-scale hydraulics is mainly affected by valves and pump efficiency [2], studies have shown that the efficiency of small-scale cylinders is proportional to its diameter, especially when the bore is less than 1 cm [3]. This indicates that monitoring the overall efficiency becomes important when designing small-scale hydraulics.

Previous efforts validated analytical models of the friction force and leakage for O-ring seals up to 300 psi [2], but it is uncertain whether these models hold at a high pressure, where high pressure is defined as 2000 psi. In addition, recent studies have shown that the power density of a tiny hydraulic system is larger than its equivalent electromechanical system only if the system operates at a pressure greater than 500 psi [4]. It is very likely that most applications of tiny hydraulics will be designed to operate at high pressure in order to achieve high overall efficiency. Examples of tiny hydraulic applications include un-tethered assistive robotics [5,6], and the envisioned hydraulic-ankle foot orthosis (HAFO) which is designed to operate at a pressure of 2000 psi [7].

In this experiment, the static leakage test showed that the volumetric efficiency is approximately 100%, and the overall efficiency is mainly dependent on force efficiency. Results also suggested that the analytical model of the friction force can be used to calculate the force efficiency up to 2000 psi. Therefore, simple analytical models of O-ring seals can be utilized to predict the overall efficiency of tiny hydraulic cylinders at high pressure.

EFFICIENCY MODEL

Friction Force

The O-ring seal friction force was modeled as [8]

$$f_s = \pi \cdot \mu_f \cdot B \cdot d \cdot E \cdot \varepsilon \cdot \sqrt{2 \cdot \varepsilon - \varepsilon^2} \tag{1}$$

where μ_f is the coefficient of friction, B is the cylinder diameter, d is the O-ring original cross section diameter, E is the modulus of elasticity of the O-ring, ε is the squeeze ratio defined as [9]

$$\varepsilon = \frac{d_s - (B - D_g)/2}{d_s} \tag{2}$$

where B is the cylinder diameter, D_g is the diameter of the piston groove, and d_s is the O-ring cross sectional diameter after being installed on the piston groove and before it is placed inside the cylinder chamber. This variable is computed as

$$d_s = d \cdot (1 - \delta) \tag{3}$$

where d is the diameter of the original cross sectional diameter, and δ is the percent decrease in O-ring original cross sectional diameter found in [10].

Cylinder Force Efficiency

For an ideal cylinder, the pressure is modeled as [2]

$$P_i = \frac{W}{A_p} \tag{4}$$

where W is the applied load and A_p is the area of the piston.

For an actual cylinder, the pressure is modeled as [2]

$$P_a = \frac{W - f_s}{A_p} \tag{5}$$

where f_s is O-ring friction force, W is the applied load, and A_p is the piston area.

Thus, the cylinder force efficiency is computed as follows [2]

$$\eta_f = \frac{P_a}{P_i} \tag{6}$$

Leakage Model

The flow rate across the O-ring rubber seal was modeled as

$$q_l = 1.495 \cdot \pi \cdot B \cdot \mu^{0.71} \cdot U_r^{1.71} \cdot \sigma_m^{-0.71} \cdot s^{0.29} \tag{7}$$

where B is the cylinder diameter, μ is the coefficient of friction, U_r is cylinder speed, σ_m is the maximum O-ring contact pressure, and s is the width of O-ring contact [11,12].

METHODS

Apparatus

Three SAE 304 steel cylinders and their respective cylinder chambers, were used in this experiment with 9, 6, and 4 mm diameters. These were machined with tight tolerances to achieve high precision [2]. Each cylinder was designed to have a length of 10 times their bore to prevent the risk of buckling [2]. A single rubber O-rings was used as the sealing method, and each size was selected to reach a squeeze ratio close to 14% with the purpose of easing the process of detecting frictional forces [2]. A linear bearing was mounted on top of each cylinder block to minimize side loadings on the rubber seals and enforce a linear piston motion [2]. White mineral oil was used as the working fluid. Two ball valves controlled the direction of the fluid flow and a needle valve regulated the descending speed of the piston. A manual hydraulic pump was used as the fluid power supply. A filter was placed at the entrance of the external reservoir. Fig. 1 shows the hydraulic schematic of the apparatus.

An aluminum bicycle wheel frame was attached to the lever of an arbor press to create a pulley system and achieve a mechanical advantage of 10:1. The arbor press was bolted to an aluminum base to prevent the press from tilting. One end of a string was attached to the wheel frame while the other was attached to a bucket used to hold the applied load. Fig. 1 includes a computer-generated drawing of the arbor press and sensor location.

A linear potentiometer (LCP12Y, ETI Systems) measured the displacement of the piston. This sensor was fixed to a vertical aluminum frame and the moving rod was attached to a lubricated slider. The velocity of piston descent was computed by calculating the slope of the position vs time graph (Fig. 2). A pressure sensor (PX300-2KGV, Omega Engineering) was placed between the cylinder chamber and the needle valve to measure the cylinder chamber pressure. A load cell (MLP-300, Transducer Techniques) measured the applied load on the cylinder. The load cell was enclosed by a customized 3-D printed case, which was attached to a lubricated slider. A USB data acquisition device (USB-6008, National Instruments) was used for digital data collection. A DC power supply provided power to the linear potentiometer and pressure sensor. A custom PCB powered the load cell and amplified the signal in order for the signals to be detected by the data acquisition device.

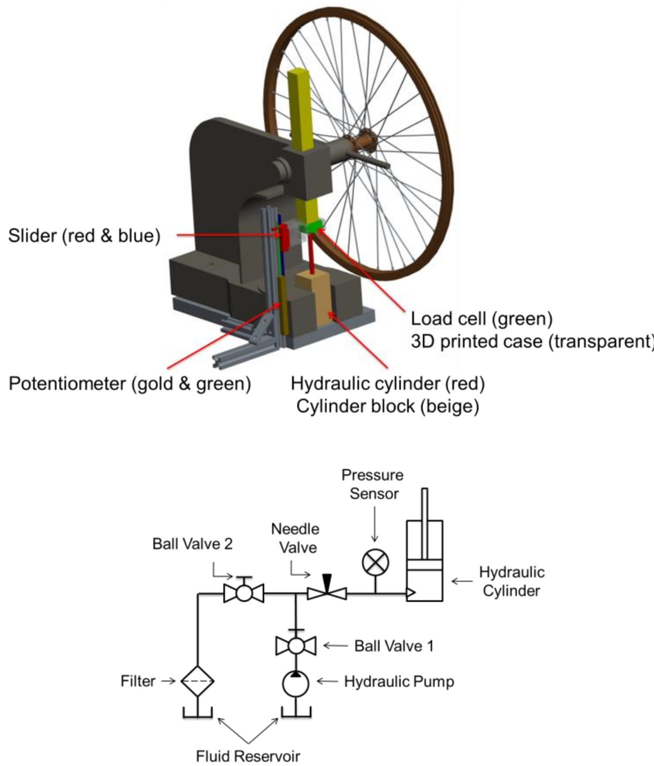

FIGURE 1. Arbor press and sensors (top), hydraulic circuit (bottom)

Protocol

The test protocol for the friction model validation was based on collecting data during steady piston descent. A set of five trials were performed for each pressure at low piston speeds (0.2-10 mm/s) and another set at high speeds (11-30 mm/s). Each trial was analyzed individually, and the average load, pressure and speed were computed for each set of five trials. Before any experimentation, the hydraulic system was bled by removing the piston and pumping fluid through the cylinder block. Afterwards, the piston was inserted into the cylinder block.

To measure O-ring friction force, the block was placed on the arbor press as illustrated in Fig. 1. A load was suspended on the pulley and this force was transmitted to the rod end of the cylinder. A manual hydraulic pump was used to lift the piston. To achieve steady piston descent, ball valve 1 was closed, the needle valve was adjusted to a desired positon, and ball valve 2 was ultimately opened (Fig. 1). Data was collected for a range of pressures between 500 and 2000 psi, and for a range of low and high speeds. Fig. 2 shows a set of data collected during piston descent.

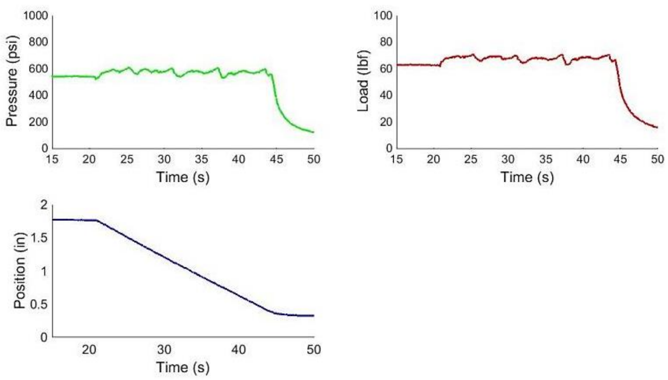

FIGURE 2. Variables measured during piston descent

A static leakage test was performed to measure the leakage across the O-ring seal. The system was initially bled the same way as was done for the friction force efficiency test. The cylinder-block assembly was positioned on the arbor press and a load was placed on the pulley to reach a chamber pressure close to 2000 psi. Fluid was pumped into the system to raise the piston and all valves were closed afterwards. Piston positions were recorded for five minutes at the 0, 12, 24 and 48 hour mark.

RESULTS

Figs. 3 through 5 show the dependence of O-ring force efficiency on chamber pressure at different descent speeds. The theoretical force efficiency is depicted as two dashed lines denoting the maximum and minimum values. The reason behind this is because the coefficient of friction can only be estimated based on how much the cylinder chamber walls are lubricated, and this surface condition can only be estimated [2]. Fig. 6 illustrates the friction force efficiency dependence on cylinder bore at high pressure.

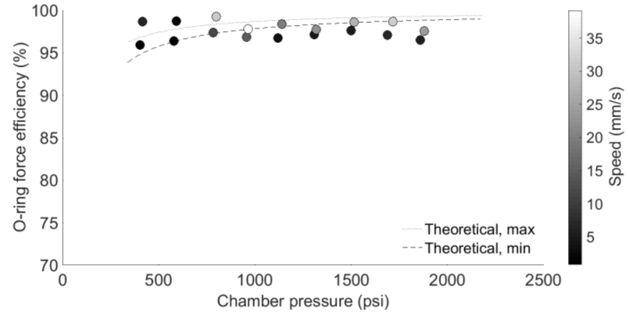

FIGURE 3. 9mm Cylinder force efficiency

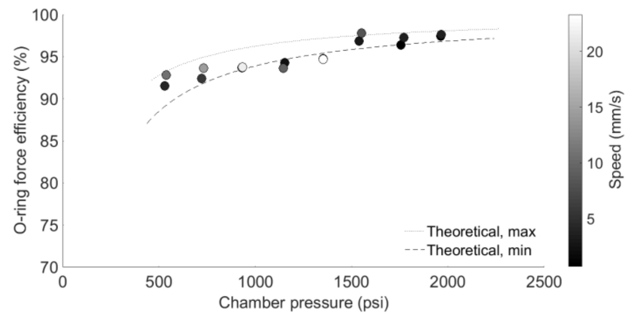

FIGURE 4. 6mm Cylinder force efficiency

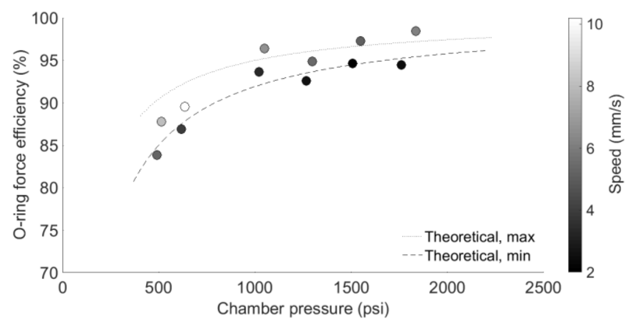

FIGURE 5. 4 mm Cylinder force efficiency

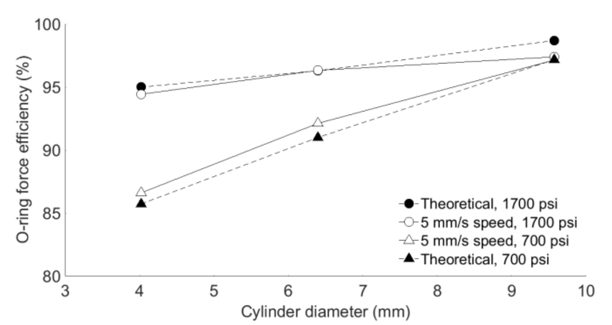

FIGURE 6. O-ring force efficiency dependency on diameter

The results of the leakage test illustrate the piston displacement over a range of 12-hour intervals. The measurement spikes are due to the digitization of the data acquisition system. The piston moved 600 microns in the first 12 hours and did not move in the following 36 hours (Fig. 7).

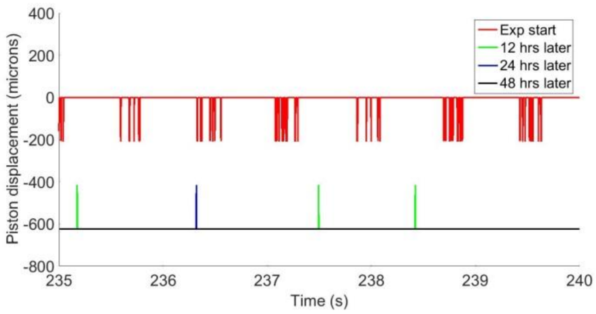

FIGURE 7. 6 mm Cylinder displacement, 1950 psi

DISCUSSION

Friction Force

Results indicate that the O-ring friction model helped to predict the measurements of the friction force efficiency model for a range of pressures between 500 and 2000 psi (Figs. 3-5). One can easily see in Fig. 5 that as the speed increases, both the chamber pressure and the force efficiency increases. As was discussed in [2], by referring to a typical Stribeck curve, as the speed increases the coefficient of friction decreases, due to a transition from the boundary to the mixed friction regime [13]. These results also suggest the need of incorporating speed in Eqn. 1 in order to have a more accurate model of the friction force for an O-ring seal.

Fig. 6 shows that the relationship between friction force efficiency and cylinder bore holds at high pressure. Note that for a constant pressure of 700 psi, the friction force efficiency increases by 11% as the bore increases from 4 to 9 mm, whereas the efficiency increases by 3% at 1700 psi. This suggests that at high pressure, such as 1700 psi or greater, piston bore has a small effect on force efficiency.

Leakage

The leakage model in Eqn. 7 could not be used to predict the leakage across the seal since it depends on the velocity of the piston, which in this case it happened to be unfeasible to measure. Thus, a static leakage test was performed instead.
Results showed that the O-ring seal can be considered as leak-free because the piston moved 600 microns during the first 12 hours, and remained steady for the following 36 hours. Therefore, the volumetric efficiency of tiny cylinders at high pressures can be approximated to be 100%, which suggests that the overall efficiency depends mainly in force efficiency.
The small piston displacement could be due to seal extrusion, which could cause the fluid to leak [10]. Fig. 8 provides a qualitative description of the effect of pressure on rubber seals and shows that at high pressure the seal starts to extrude through the clearance gap. Handbook recommends using an O-ring with higher hardness or the use of anti-extrusion device in order to mitigate seal extrusion [10].

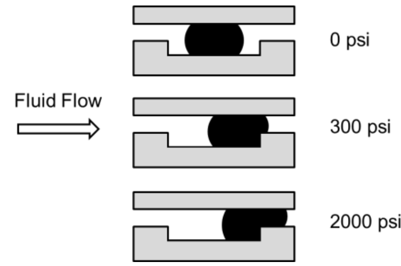

FIGURE 8. Effects of pressure on O-ring seals

CONCLUSION

The results from this study showed that the analytical models of O-ring seals can be used to predict the overall efficiency of small-scale hydraulic systems for pressures between 500 and 2000 psi. It also illustrated the need of incorporating velocity into the friction force model in order to improve the accuracy of the model. In addition, the force efficiency dependency on cylinder bore becomes insignificant at a pressure greater than 1700 psi. The leakage test showed that the volumetric efficiency is approximately 100%. Therefore, the friction force model can be used to predict the overall efficiency of tiny hydraulics at high pressure.

ACKNOWLEDGEMENT

This project was supported by the University of Minnesota's Undergraduate Research Opportunities Program and by the Center for Compact and Efficient Fluid Power.

REFERENCES

[1] Durfee, W. and Sun, Z., 2009. “Fluid Power System Dynamics”.

[2] Xia, J. and Durfee, W.K., 2014. “Experimentally validated models of O-ring seals for tiny hydraulic cylinders”. In ASME/Bath 2014 Symposium on Fluid Power & Motion Control.

[3] Xia, J. and Durfee, W., 2013. “Analysis of small-scale hydraulic actuation systems”. ASME Journal of Mechanical Design, 135(9):091001 -1-091101-11

[4] Durfee, W.K., Xia, J., and Hsiao-Wecksler, E., 2011. “Tiny hydraulics for powered orthotics”. IEEE International Conference Rehabilitation Robotics, pp 1-6.

[5] A. Zoss, Kazerooni, H, 2005. “Architecture and Hydraulics of a Lower Extremity Exoskeleton”, 2005 ASME International Mechanical Engineering Congress and Exposition

[6] De Asha, A. R., 2015. "Biomechanical adaptations of lower-limb amputee-gait: Effects of the echelon hydraulically damped foot. Segmental kinetic and kinematic response to hydraulically damped prosthetic ankle-foot components in unilateral, tans-tibial amputees". Thesis.
[7] Neubauer, B., Nath, J. and Durfee, W. 2014. "Design of a portable hydraulic ankle-foot orthosis." In Annual International Conference of the IEEE Engineering in Medicine and Biology Society.
[8] Al-Ghathian, F. M. M., and Tarawneh, M. S., 2005. "Friction forces in o-ring sealing". American Journal of Applied Sciences, 2(3), pp. 626–632.
[9] Xia, J., and Durfee, W. K., 2011. "Modeling of tiny hydraulic cylinders". In 52nd National Conference of Fluid Power, pp. 1–5.
[10] Hannifin, P., 2007. Parker O-Ring Handbook. Parker Hannifin Corp., Lexington, KY.
[11] Karaszkiewicz, A., 1988. "Hydrodynamic lubrication of rubber seals for reciprocating motion; leakage of seals with an o-ring". Tribology International, 21(6), pp. 361-367.
[12] Karaszkiewicz, A., 1990. "Geometry and contact pressure of an o-ring mounted in a seal groove". Ind. Eng. Chem. Res., 29, pp. 2134–2137.
[13] Dowson, D., 1998. History of Tribology. Professional Engineering Publishing, London and Bury St Edmunds, UK.